Characterization of Microstrip Waveguides in Silicon up to 80 GHz

Daniel Kehrer[1,2], Josef Winkler[2], Harald Tischer[1], Hans-Dieter Wohlmuth[1], Werner Simbürger[1], Arpad L. Scholtz[2]

[1]INFINEON Technologies AG, Corporate Research, Otto-Hahn-Ring 6, D-81739 Munich, Germany, Phone: +49 89 234-48490, Fax.: +49 89 234-47069, E-Mail: daniel.kehrer@infineon.com

[2]Technical University Vienna, Institute of Communications and Radio-Frequency Engineering Gußhausstraße 25/389, A-1040 Vienna, Austria

Abstract –

A monolithically integrated microstrip waveguide in a 0.5 μm, Si bipolar technology is presented. This single microstrip line is a common type of on chip interconnnect. The waveguide is characterized by S-parameter measurement in a frequency range from 100 MHz to 80 GHz. After deembedding the characteristic impedance, propagation constant and telegraphers equation transmission parameter are extracted. Measurement Results are compared to simulation results in detail.

Keywords – **microstrip line, microwave guides, MMIC circuit design.**

I. Introduction

Nowadays silicon-based monolithic microwave integrated circuits tend to very high frequencies. The designer has to pay attention to interconnect design which influences the performance of ICs significantly [1]. The connection between circuit core and pads are very long on-chip interconnects and in many cases realized as microstrip line. The interconnect should meet many demands like low loss or to match a certain Impedance. This paper presents a full characterization of a single microstrip line to demonstrate the electrical behaviour of such interconnects.

Recent papers have presented several methods for characterizing transmission lines by the characteristic impedance [2], [3]. An ideal transmission line is characterized completely by the characteristic impedance Z_0 and the propagation constant γ. The characterization of the microstrip line is based on S-Parameter measurement [4] with a thru-reflect-line (TRL) calibration [3], [5].

This paper shows an accurate characterization of a monolithically integrated microstrip waveguide in a 0.5 μm, Si bipolar technology up to 80 GHz. In Section II the technology and the microstrip line geometries are described. For accurate measurement results in Section III the deembedding procedure is explained. Section IV discusses the theory of S-parameter based transmission line characterization. In Section V the experimental results of the microstrip line are presented and compared to simulation results in detail.

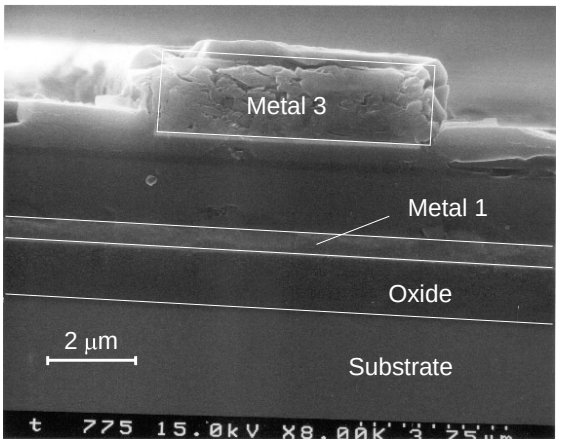

Fig. 1. Cross section of the monolithically integrated microstrip line. Microstrip line is Metal 3. Ground Plane is Metal 1

II. Silicon-based Technology and Metallization

A detailed cross-section of the 3 layer metallization is shown in Fig. 2. The conductor material is standard AlSiCu and has a conductivity of $\sigma = 33\,\mathrm{S}/\mu\mathrm{m}$. The metal layers are embedded in Silicondioxide SiO_2 with a relative permittivity of $\varepsilon_r = 3.9$. The passivation is formed by a airproof protection coat and consists of Siliconnitride Si_3N_4 and has an $\varepsilon_r = 7.5$. The substrate is a p^- doped Silicon with a conductivity of $\sigma = 12.5\,\mathrm{S/m}$ ($8\,\Omega cm$).

The microstrip line is realized in Metal 3 as signal line and Metal 1 as ground plane. Metal 2 is not used. A cross section of the microstrip waveguide is illustrated in Fig. 1. The microstrip line has a width of $w = 6\,\mu$m and a conductor-height of $T = 1.4\,\mu$m (Metal 3 in Fig. 2). The spacing between Ground plane (Metal 1) and conductor is $H = 2.9\,\mu$m. The width to height ratio of the microstrip is $W/H = 2.07$.

III. Deembedding

To extract the electrical characteristic of the microstrip line from the measurement data, deembedding test structures are necessary. A calibration method with "short" and "open" test structures applies correct characterization only at low frequencies. To get accurate results at high frequen-

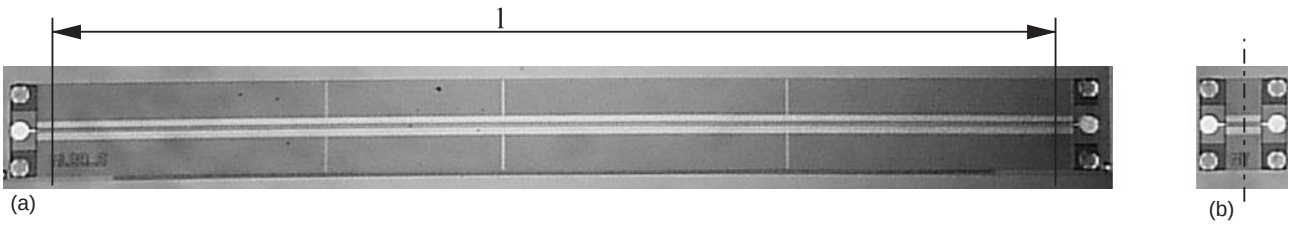

Fig. 3. High frequency waveguide test structures layout. (a) Microstrip line test structure. (b) Deembedding test structure.

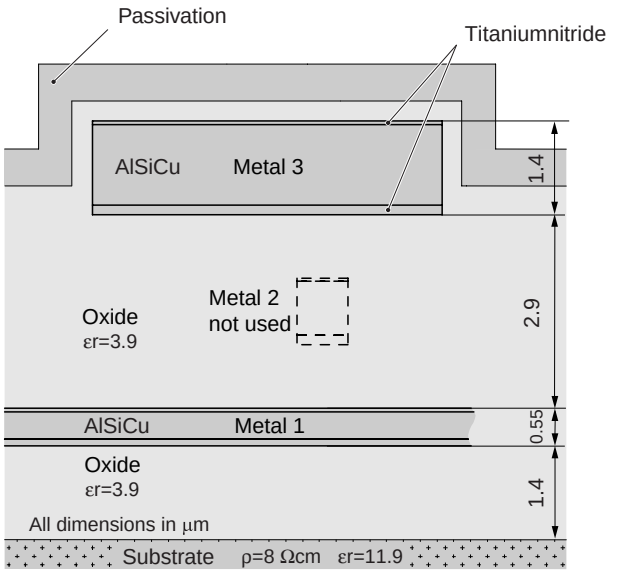

Fig. 2. Detailed schematic cross section of the metallization.

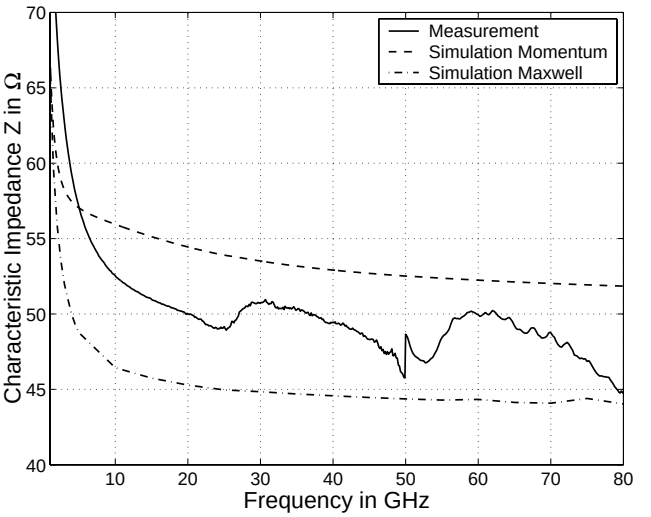

Fig. 4. Measured and simulated characteristic impedance versus frequency of the $W/H = 6\mu\text{m}/2.9\mu\text{m}$ microstrip line.

cies up to 80 GHz, a thru-reflect-line (TRL) calibration is required. Fig. 3(a) shows a chip micrograph of the microstrip line teststructure with $40\,\mu m$ high frequency pads on left and right side to contact with ground-signal-ground probes. The total length of the microstrip line teststructure is $2800\,\mu m$. Fig. 3(b) shows the chip micrograph of the thru-reflect-line calibration test structure for deembedding.

If two-ports are connected in cascade the system can be practically defined by the transmission matrix (T-matrix). The measurement data is in the form of S-parameter and therefore we need the equations to get the T-matrix of a two-port.

$$\mathbf{T} = \frac{1}{S_{21}} \begin{pmatrix} 1 & -S_{22} \\ S_{11} & S \end{pmatrix} \tag{1}$$

where $S = \det(\mathbf{S}) = S_{11}S_{22} - S_{12}S_{21}$ is the determinante of the S-matrix. The T-matrix of the microstrip line test structure in Fig. 3(a) can be written as

$$\mathbf{T}_{Measure} = \mathbf{T}_{Pad_{left}} \cdot \mathbf{T}_{Line} \cdot \mathbf{T}_{Pad_{right}} \tag{2}$$

with T-matrix of the pads on the left and right side. On the other hand the T-matrix of the deembedding test structure in Fig. 3(b) can be written as

$$\begin{aligned} \mathbf{T}_{Pad} &= \mathbf{T}_{Pad_{left}} \cdot \mathbf{T}_{Pad_{right}} \\ \mathbf{T}_{Pad_{left}} &= \mathbf{T}_{Pad_{right}} = \sqrt{\mathbf{T}_{Pad}} \end{aligned} \tag{3}$$

With (2) and (3) we can extract the T-matrix of the microstrip line $\mathbf{T}_{Line}$ as follows

$$\mathbf{E} \cdot \mathbf{T}_{Line} \cdot \mathbf{E} = \mathbf{T}^{-1}_{Pad_{left}} \cdot \mathbf{T}_{Measure} \cdot \mathbf{T}^{-1}_{Pad_{right}} \tag{4}$$

where $\mathbf{E}$ is the unity matrix. After extracting $\mathbf{T}_{Line}$ we convert to the familiar S-parameter of the deembedded line.

$$\mathbf{S} = \frac{1}{T_{11}} \begin{pmatrix} T_{21} & T \\ 1 & -T_{12} \end{pmatrix} \tag{5}$$

where $T = \det(\mathbf{T})$.

IV. Parameter Extraction

After deembedding we have extracted the S-parameter of the transmission line which describe the full electrical behaviour. A figure of merit is the characteristic impedance Z and the propagation constant $\gamma = \alpha + j\beta$ where α is the attenuation constant and β is the phase constant. The S-parameter measured from a lossy unmatched transmission line with characteristic impedance Z and propagation constant γ in a Z_0 impedance system are [4]

$$\mathbf{S} = \frac{1}{D_s} \begin{pmatrix} (Z^2 - Z_0^2)\sinh\gamma l & 2ZZ_0 \\ 2ZZ_0 & (Z^2 - Z_0^2)\sinh\gamma l \end{pmatrix} \tag{6}$$

where $D_s = 2ZZ_0\cosh\gamma l + (Z^2 + Z_0^2)\sinh\gamma l$. The S-matrix can be solved in γ and Z. The product γl in terms of the

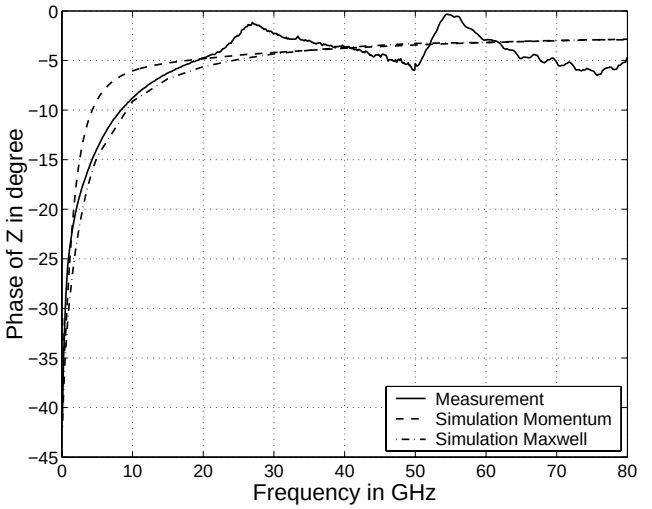

Fig. 5. Measured and simulated phase of the characteristic impedance versus frequency.

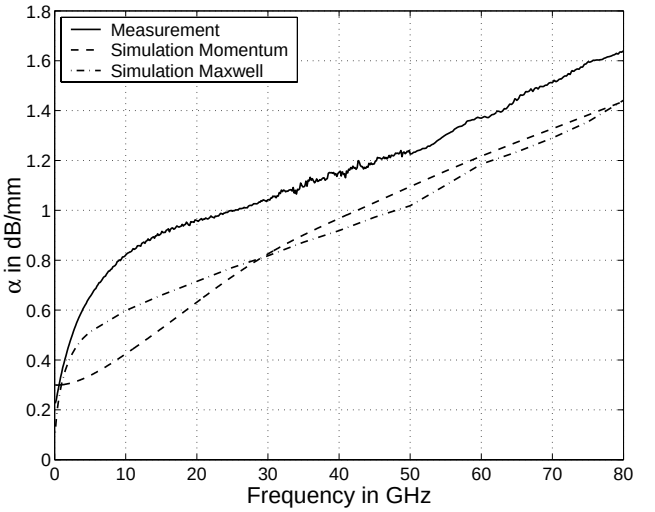

Fig. 6. Measured and simulated attenuation per mm versus frequency of the $W/H = 6\mu\text{m}/2.9\mu\text{m}$ microstrip line.

S-parameter can be written as

$$\gamma l = -\ln\left(\frac{1-S_{11}^2+S_{21}^2}{2S_{21}} \pm \sqrt{\frac{(S_{11}^2-S_{21}^2+1)^2-(2S_{11})^2}{(2S_{21})^2}}\right) \quad (7)$$

where l is the length of the deembedded line (Fig. 3). The characteristic impedance Z in terms of the S-parameter can be written as

$$Z = Z_0\sqrt{\frac{(1+S_{11})^2-S_{21}^2}{(1-S_{11})^2-S_{21}^2}} \quad (8)$$

The solutions of (7) and (8) must be chosen to be physically real.

A fundamental characteristic parameter of a waveguide is the attenuation constant α. It represents dielectric and ohmic losses of the waveguide. α can be calculated with (9) where γ was derived with (7).

$$\alpha = \text{Re}\{\gamma\} \quad (9)$$

Not only the characteristic impedance and the propagation constant must be observed: also the classical telegraphers equation transmission parameters (R, L, G and C) give a fundamental insight. These distributed circuit paramters describe per length unit and are not lumped element values. From the well known relation of a lossy transmission line

$$\gamma = \sqrt{(R+j\omega L)\,(G+j\omega C)} \quad (10)$$

$$Z = \sqrt{\frac{R+j\omega L}{G+j\omega C}} \quad (11)$$

we extract the Telegraphers Equation transmission parameters (R, L, G and C) as follows:

$$\begin{aligned} R &= \text{Re}\{\gamma Z\} \\ L &= \text{Im}\{\gamma Z\} \end{aligned} \quad (12)$$

$$\begin{aligned} G &= \text{Re}\{\gamma/Z\} \\ C &= \text{Im}\{\gamma/Z\} \end{aligned}$$

V. Experimental Results

The microstrip line was designed to match 50 Ω. Fig. 4 shows measured and simulated characteristic impedance Z versus frequency. The unsteady peak at 50 GHz is due to the different measurement setup in the range from 50 MHz to 50 GHz and from 50 GHz to 80 GHz.

The characteristic impedance Z is separated into the absolute value (Fig. 4) and the phase (Fig. 5) as a function of frequency. At frequencies lower than 15 GHz the magnetic- and electric-field is not in phase (-40° at 50 MHz) and the microstrip line carries a slow wave mode. At high frequencies the microstrip line exhibits a quasi-TEM mode.

At frequencies where the microstrip line length is a multiple of the half wave length the S-parameter measurement is very sensitive [8]. In our case this effect causes measurement errors at 27 GHz and 54 GHz. Due tue the measurement errors at this frequencies the extracted characteristic impedance Z, the characteristic series resistance R and the characteristic capacitance C are strongly influenced.

Fig. 6 shows the measured attenuation compared to simulations with Maxwell Field Simulator [6] and Momentum Field Simulator [7]. The small deviation between measurement and simulation verify the parameter extraction from the S-parameter measurement. As expected the attenuation constant increases with frequency. The increasing attenuation can be explained with the skin effect and the polarization losses of the dielectric.

Fig. 7 shows the measured and simulated characteristic series resistance slightly increasing with frequency. The calculated series resistance of 3.8 Ω/mm matches the measurement at low frequencies. The skin-depth at 20 GHz is 0.6 μm which is about a half of the conductor height T. The series resistance is very sensitive to measurement errors of

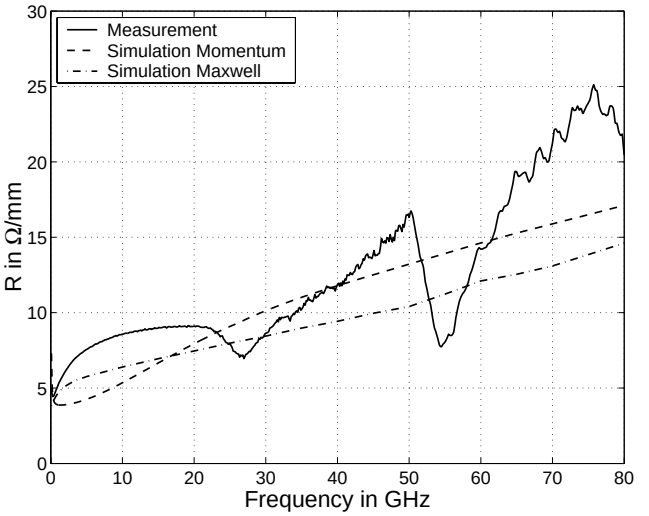

Fig. 7. Measured and simulated characteristic series resistance versus frequency. The calculated series resistance of $3.8\,\Omega$/mm matches the measurement at low frequencies.

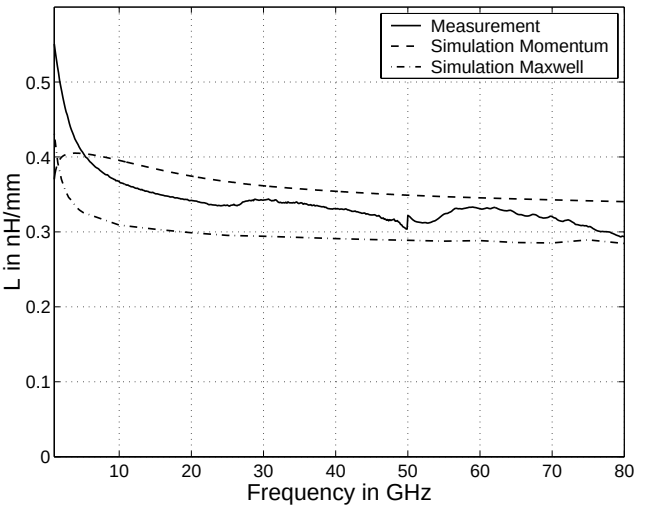

Fig. 8. Measured and simulated characteristic inductance versus frequency of the $W/H = 6\mu$m$/2.9\mu$m microstrip line.

the phase of Z.

The characteristic conductance is very sensitive to measurement errors of the phase of Z. The values of the characteristic conductance over frequency is in the same range as the measurement error and therefore not illustrated.

Fig. 8 illustrates the measured and simulated characteristic inductance versus frequency of the microstrip line. The inductance is slightly decreasing from DC up to 10 GHz due tue the current crowding in the conductor. At frequencies greater than 10 GHz the inductance is relatively constant.

The characteristic capacitance plot in Fig. 9 shows a high capacitance at low frequencies and a relatively constant capacitance at frequencies higher than 10 GHz. The capacitance from DC to 10 GHz is reduced because the propagation mode changes from a slow wave mode to a quasi-TEM mode.

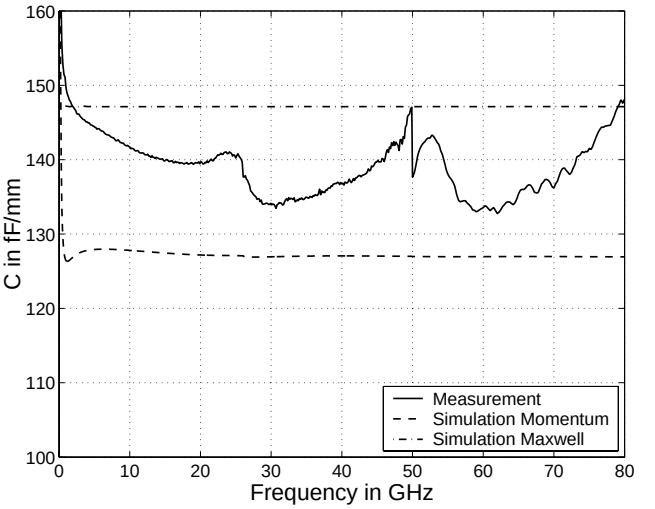

Fig. 9. Measured and simulated characteristic capacitance versus frequency of the $W/H = 6\mu$m$/2.9\mu$m microstrip line.

VI. Conclusion

We have presented an accurate characterization of a microstrip line on silicon up to 80 GHz. With the presented deembeding algorithm the electrical behaviour of the microstrip line can be extracted. Measurement and simulation of the attenuation shows good agreement over the whole frequency range. The extracted parameters are very sensitive at frequencies where the microstrip line length is a multiple of the half wavelength. The characteristic impedance, propagation constant and telegraphers equation transmission parameter of the microstrip line are presented to give a fundamental insight.

References

[1] A. Deutsch, G. V. Kopcsay, P. J. Restle, H. H. Smith, G. Katopis, W. D. Becker, P. W. Coteus, C. W. Surovic, B. J. Rubin, R. P. Dunne, T. Gallo, K. A. Jenkins, L. M. Terman, R. H. Dennard, G. A. Sai-Halasz, B. L. Krauter and D. R. Knebel, "When are Transmission-Line Effects Important for On-Chip Interconnections?", *IEEE Trans. on Microwave Theory and Techn.*, vol. 45, n. 10, pp. 1917 –1920, October 1997.

[2] D. F. Williams and B.K. Alpert, "Characteristic Impedance of Microstrip on Silicon", in *Electrical Performance of Electronic Packaging*, pp. 181–184, 1999.

[3] A. Bracale, D. Pasquet, J.L. Gautier, N. Fel, V. Ferlet and J.L. Pelloie, "A new method for characteristic impedance determination on lossy substrate", *Microwave Symposium Digest*, vol. 3, pp. 1481 –1484, 2000.

[4] W.R. Eisenstadt and Y. Eo, "S-parameter-based IC interconnect transmission line characterization", *IEEE Trans. Comp.*, vol. 15, pp. 483–490, August 1992.

[5] D. F. Williams and B. Marks, "Accurate Transmission Line Characterization", *IEEE Microwave and Guided Wave Lett.*, vol. 3, n. 8, pp. 247–249, August 1993.

[6] Ansoft Corporation, *Maxwell 2D and 3D Field Simulator*, Ansoft Corporation, 1993.

[7] HP, *User's Reference Guide for Momentum Field Simulator*, HP Corporation, 1994.

[8] Y.C. Shih and K.S. Kong, "Accurate broadband characterization of transmission lines", *Microwave Symposium Digest*, vol. 2, pp. 933 –936, 1998.